Geophysical Journal International

Geophys. J. Int. (2017) **209,** 1906–1912
Advance Access publication 2017 March 30
GJI Geodynamics and tectonics

doi: 10.1093/gji/ggx136

ITRF2014 plate motion model

Zuheir Altamimi,[1] Laurent Métivier,[1] Paul Rebischung,[1] Hélène Rouby[1] and Xavier Collilieux[2]

[1]*IGN LAREG, Université Paris Diderot, Sorbonne Paris Cité, F*75205 *Paris CEDEX* 13*, France. E-mail: zuheir.altamimi@ign.fr*
[2]*Ecole Nationale des Sciences Géographiques, F-*77455 *Marne la Vallée, France*

Accepted 2017 March 29. Received 2017 March 26; in original form 2016 December 6

SUMMARY

For various geodetic and geophysical applications, users need to have access to a plate motion model (PMM) that is consistent with the ITRF2014 frame. This paper describes the approach used for determining a PMM from the horizontal velocities of a subset of the ITRF2014 sites away from plate boundaries, Glacial Isostatic Adjustment regions and other deforming zones. In theory it would be necessary to include in the inversion model a translational motion vector (called in this paper origin rate bias, ORB) that would represent the relative motion between the ITRF2014 origin (long-term averaged centre of mass of the Earth as sensed by SLR) and the centre of tectonic plate motion. We show that in practice, the magnitude of the estimated ORB is strongly dependent on the selection of ITRF2014 sites used for the PMM adjustment. Its Z-component can in particular range between 0 and more than 1 mm yr^{-1} depending on the station network used, preventing any geophysical interpretation of the estimated value. Relying on rigorous statistical criteria, the site selection finally adopted for the ITRF2014-PMM adjustment leads to a relatively small ORB (0.30 ± 0.18 mm yr^{-1} in the Z-component), which is statistically insignificant at the 2-sigma level, but also according to an F-ratio test. Therefore we opted for an ITRF2014-PMM without estimating the ORB, which in turn accommodates geodetic applications that require access to the ITRF2014 frame through pure plate rotation poles.

Key words: Plate motion; Reference systems.

1 INTRODUCTION

Quantifying plate motion is essential to understanding the mechanism of plate tectonics and its implications for geologic processes at plate boundaries, including how these processes relate to earthquakes and volcanic activity. Space geodesy measurements that started in the late seventies today can quantify plate movements at the level of sub-millimetre per year. The International Terrestrial Reference Frame (ITRF), based on a combination of station positions and velocities provided by space geodetic techniques (VLBI, SLR, GNSS and DORIS), permits the determination of precise absolute and relative motions of major tectonic plates. Each time a new release of the ITRF is published, a corresponding and consistent plate motion model (PMM) is proposed in order to satisfy the user need for various geodetic and geophysical applications. One of the practical geodetic applications to be cited here is the fact that the ITRF is used as the standard in national and continental reference frame implementation where the rotation pole of a given plate is often part of their definitions. This is the case, for instance, for the European Terrestrial Reference System 89 (ETRS89) which is intimately linked to the International Terrestrial Reference System by a transformation formula that involves the Eurasian angular velocity (Altamimi & Boucher 2002). Another example is the NA12 reference frame developed by Blewitt *et al.* (2013) for crustal deformation studies in North America, where the authors adjusted an Euler pole for the North American plate that is statistically not far from the ITRF2008-PMM estimate (Altamimi *et al.* 2012). A further example is the North America reference frame, NAM08, which uses the ITRF2008-PMM rotation pole for North America, with the translational vector (discussed below) set to zero, developed for the geodetic products generated from Plate Boundary Observatory GPS data (Herring *et al.* 2016).

It is worth recalling here that the ITRF frames satisfy, implicitly, the no-net-rotation (NNR) condition applied to the Earth's surface, since ITRF2000 (Altamimi *et al.* 2002) was initially aligned to the global PMM NNR-NUVEL-1A (Argus & Gordon 1991; DeMets *et al.* 1990; DeMets *et al.* 1994) which also satisfies that condition. Note that after ITRF2000, the subsequent ITRF solutions were successively aligned to each other in orientation and orientation time evolution. As a consequence, we can show that, in theory, the ITRF2008-PMM (Altamimi *et al.* 2012) should be consistent with the ITRF2014 and therefore there would be no need to estimate an ITRF2014-PMM. However, as ITRF2014 includes more sites (especially GNSS sites) than ITRF2008 and five additional years

of data, we expect now to derive a more robust PMM compared to ITRF2008-PMM.

Extensive analysis and discussions were published in Altamimi *et al.* (2012), regarding in particular comparisons with existing geological PMMs, such as NNR-NUVEL-1A (Argus & Gordon 1991) and NNR-MORVEL56 (Argus *et al.* 2011), derived from MORVEL (DeMets *et al.* 2010), and GEODVEL (Argus *et al.* 2010), that are not worth repeating here. The main points of this article are the provision of a robust ITRF2014-PMM, consistent with the ITRF2014 frame, as well as the evaluation of the pertinence of the translational motion vector that we call here the Origin Rate Bias (ORB).

The inversion models with and without the ORB are recalled in Section 2, and the main criteria of site selection are described in Section 3. Section 4 is devoted to data analysis, with detailed discussion of the impact of the network selection effect on the estimation of the ORB components. The final ITRF2014-PMM is presented and discussed in Section 5.

2 INVERSION MODELS

The basic equation used to estimate an angular velocity (or rotation pole), ω_p, of a plate p, involves for point i located on the rigid part of that plate, its velocity, $\dot{X}_i$, and its position vector X_i:

$$\dot{X}_i = \omega_p \times X_i \tag{1}$$

When estimating multiple plate rotation poles together, from a global velocity field, we can add a translational motion component to eq. (1), called here an origin rate bias (ORB), as investigated by Argus *et al.* (2010), Kogan & Steblov (2008), and Altamimi *et al.* (2012), so that

$$\dot{X}_i = \omega_p \times X_i + \dot{T} \tag{2}$$

Ideally, if the ITRF2014 selected sites were perfectly and regularly distributed to sample and discretize all tectonic plates, $\dot{T}$ would represent the translational motion between the ITRF2014 origin (long-term averaged centre of mass of the Earth as sensed by SLR) and the geometric centre of tectonic plate motion. The latter corresponds to the residual centre of surface lateral figure (CL) as defined by Blewitt (2003). However, as will be discussed in this paper, the value of the estimated ORB strongly depends on the selection of ITRF2014 sites used for the PMM adjustment.

3 SITE SELECTION

We followed similar, but enhanced criteria for the selection of ITRF2014 sites as for the ITRF2008-PMM (Altamimi *et al.* 2012) based on the following conditions: (1) the time-span of observations per site had to be longer than 3 yr, (2) the sites should not be affected by post-seismic deformations as modelled in the ITRF2014 processing (Altamimi *et al.* 2016), (3) the sites were to be at least 100 km from the Bird (2003) plate boundaries, outside deformation areas following the criteria of Argus & Gordon (1996) and the strain map of Kreemer *et al.* (2014), and far from Glacial Isostatic Adjustment (GIA) regions (as defined below), (4) the normalized post-fit velocity residuals (raw residuals divided by their *a priori* uncertainties) had to be smaller than 3, and (5) the raw residuals had to be less than 1 mm yr^{-1}.

Concerning condition 1, we believe that 3 yr represent the minimum time-span for the estimation of a reliable station velocity and to mitigate possible biases due to periodic variations (Blewitt & Lavallée 2002), although annual and semi-annual signals were originally adjusted during the ITRF2014 processing (Altamimi *et al.* 2016).

In order to satisfy condition 3, we excluded sites located in regions that were covered by ice sheets during the last glacial maximum and which should theoretically show large GIA induced vertical velocities. For simplicity, we call these regions 'GIA regions'. We adopted the Australian National University (ANU) GIA model of Lambeck *et al.* (2014, 2017) to retain sites that have predicted vertical velocities less than 0.75 mm yr^{-1}. This site selection is also globally consistent with, although slightly more stringent than with the ICE6G GIA model of Peltier *et al.* (2015), using the same criteria. We did not take into account GIA horizontal velocity predictions in our selection, given the results of our previous study (Altamimi *et al.* 2012). However, we performed a few GIA modelling tests based on the ANU ice history model with various viscosity profiles in order to evaluate the possible impact of GIA deformations on horizontal velocities outside the so-called GIA regions. We found that GIA, depending on modelling parameters, may induce horizontal velocities far from GIA regions at a level up to 3–4 mm yr^{-1}, in the worst case scenario. Given these results we believe that users should be aware that ITRF2014-PMM, as all past geodetic PMM, may be slightly but significantly contaminated by GIA, depending on site locations. Therefore it would not be optimal to subtract PMM predictions from a velocity field in order to investigate GIA deformations. Finally, we did not exclude Antarctica sites from our selection in order to supply a rotation pole for that plate, and because our GIA tests showed that the Euler pole could be biased by GIA effects only marginally.

Condition 4 is the usual and commonly accepted statistical criteria that allows detecting data outliers at 99.7 per cent confidence limits. Having more sites in ITRF2014 network, compared to past solutions, condition 5 is adopted in order to derive the most robust and enhanced PMM, compared to the ITRF2008-PMM.

4 DATA ANALYSIS

When selecting a subset of sites from the global ITRF2014 SINEX file, together with their associated full variance covariance terms, the reference frame effect (Sillard & Boucher 2001) is altered by the change of the network and has to be re-specified using the so-called inner constraints. The latter have the algebraic property to precisely specify the reference frame effect within the variance covariance matrix, without changing the estimates (positions and velocities) of the solution. Therefore we applied this type of inner constraints to the variance covariance matrix each time we changed the network of the selected sites, using the appropriate eq. (A15) of Altamimi *et al.* (2002).

Applying the inversion model of eq. (2), and an iterative process, we found in total 318 sites located on 11 plates (versus 206 sites and 14 plates for ITRF2008-PMM) that satisfy all five selection criteria described in the previous section. We discarded the Amurian, Sunda and Caribbean plates for their significant seismic and post-seismic activities, but also for their small number of available geodetic sites. Using the velocity field of the 318 sites with the corresponding inner-constrained variance covariance matrix, we found the following components of the ORB: 0.19(±0.17), 0.20(±0.19), 0.85(±0.18), for $\dot{T}_X$, $\dot{T}_Y$, $\dot{T}_Z$ mm yr^{-1}, respectively.

We then performed several inversion tests in order to evaluate and quantify the impact of the network effect of the selected velocity field on the estimated parameters. During this process, we came across a particular case where the Z-translation rate ($\dot{T}_Z$) decreased by 43 per cent, namely it dropped from 0.85 to

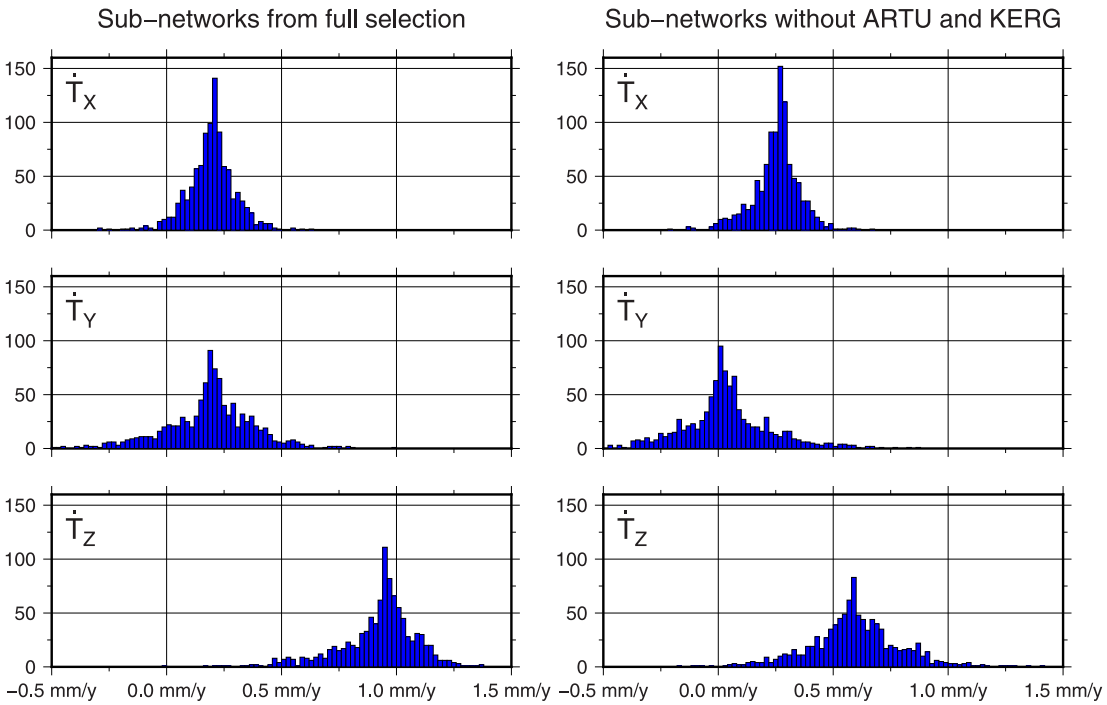

Figure 1. Histograms of the ORB components obtained from 1000 randomly selected velocity fields, with (left) and without (right) ARTU and KERG.

0.48(±0.20) mm yr^{-1}, while ($\dot{T}_Y$) vanished to zero, if just two sites (ARTU - Arti Geophysical Observatory, Russia, and KERG - Kerguelen Island) are rejected from the ensemble of 318 sites; $\dot{T}_X$ is only marginally affected. We believe that this result is a convincing and telling example of the significant impact of the network effect on the estimated parameters, and in particular $\dot{T}_Z$. We think that this strong dependency of the estimated ORB on the selected network prevents any geophysical interpretation of its estimated value. To illustrate this further, we selected 1000 random subnetworks, each of which contains randomly between 150 and 318 sites (or 316 sites when ARTU and KERG are discarded). Fig. 1 illustrates the histograms of the three ORB components obtained from the corresponding 1000 velocity fields with (left) and without (right) ARTU and KERG. We can see from that figure the scatter of the resulting ORB components, especially $\dot{T}_Y$ and $\dot{T}_Z$, but also the shifts of these two components (unlike $\dot{T}_X$) when ARTU and KERG are not considered. These results show that (1) $\dot{T}_X$ is only slightly affected by the network selection, with an approximate value around 0.20 mm yr^{-1}, (2) $\dot{T}_Y$ and $\dot{T}_Z$ are volatile and are heavily impacted by the network effect, which prevents any geophysical interpretation of their values, and (3) the velocities of two points (ARTU and KERG) are enough to drag $\dot{T}_Y$ and $\dot{T}_Z$ considerably, which likely reflects an inconsistency of their velocities with the rest of their respective plate velocity fields. These findings led us to adopt an additional site selection criterion for the final ITRF2014-PMM adjustment, so as to keep only sites showing good statistical agreement with their respective plate velocity fields.

To that end, we performed successive global inversions estimating individual rotation poles of all plates together, using the model of eq. (1), and iteratively rejected sites where the normalized residual of any of the two horizontal components exceeded 3.0, and ended up by rejecting 21 sites where the two particular sites (ARTU and KERG, see their locations in Fig. 2) were part of the rejected sites. We then applied the model of eq. (2) to the remaining filtered network of 297 sites and found the following ORB components: 0.20(±0.15), 0.00(±0.18), 0.30(±0.18) mm yr^{-1}, for $\dot{T}_X$, $\dot{T}_Y$, $\dot{T}_Z$, respectively. Fig. 2 displays the site residuals of the full set of the selected 318 sites (top panel) and the filtered network after rejecting 21 sites (bottom panel). Inspecting that figure, one can easily see that the residuals of both models show similar features and magnitudes, suggesting that the large Z-component (and to some extent the Y-component) of the ORB found when using the 318 sites are artificially inflated by the 21 sites (and especially by ARTU and KERG) whose velocities are likely impacted by some local phenomena.

We then adopted the remaining 297 sites as our final network of velocity field for the determination of the ITRF2014-PMM where 57 per cent of them are located in the Eurasian (97 sites) and North American (72 sites) plates. Note that the locations of the rejected 21 sites do not significantly modify the overall site distribution over the involved plates (compare top and bottom panels of Fig. 2).

5 ITRF2014 PLATE MOTION MODEL

In order to select the final ITRF2014-PMM, that is, with or without the ORB, we based our judgement on sound statistical considerations. We consider that from the pure statistical point of view, the estimated ORB components [0.20(±0.15), 0.00(±0.18), 0.30(±0.18) mm yr^{-1} for $\dot{T}_X$, $\dot{T}_Y$, $\dot{T}_Z$, respectively] are not significantly far from zero at the 2-sigma level. We further computed an F-ratio test using (Nocquet *et al.* 2001)

$$F = \frac{[\chi^2(p1) - \chi^2(p2)]/(p1 - p2)}{\chi^2(p2)/p2} \tag{3}$$

where χ^2 is the square sum of the normalized residuals (that is minimized by the least squares adjustment), $p1 = 561$ and $p2 = 558$ are the degrees of freedom (number of observations minus the number of unknowns) without and with the ORB, respectively.

Computing the F quantity using eq. (3), we found 1.368, while the expected value of $F(p1 - p2, p2)$ Fisher-Snedecor's distribution is 2.621, for a risk level corresponding to 95 per cent confidence level. The F-ratio test indicates clearly that the estimated ORB is not

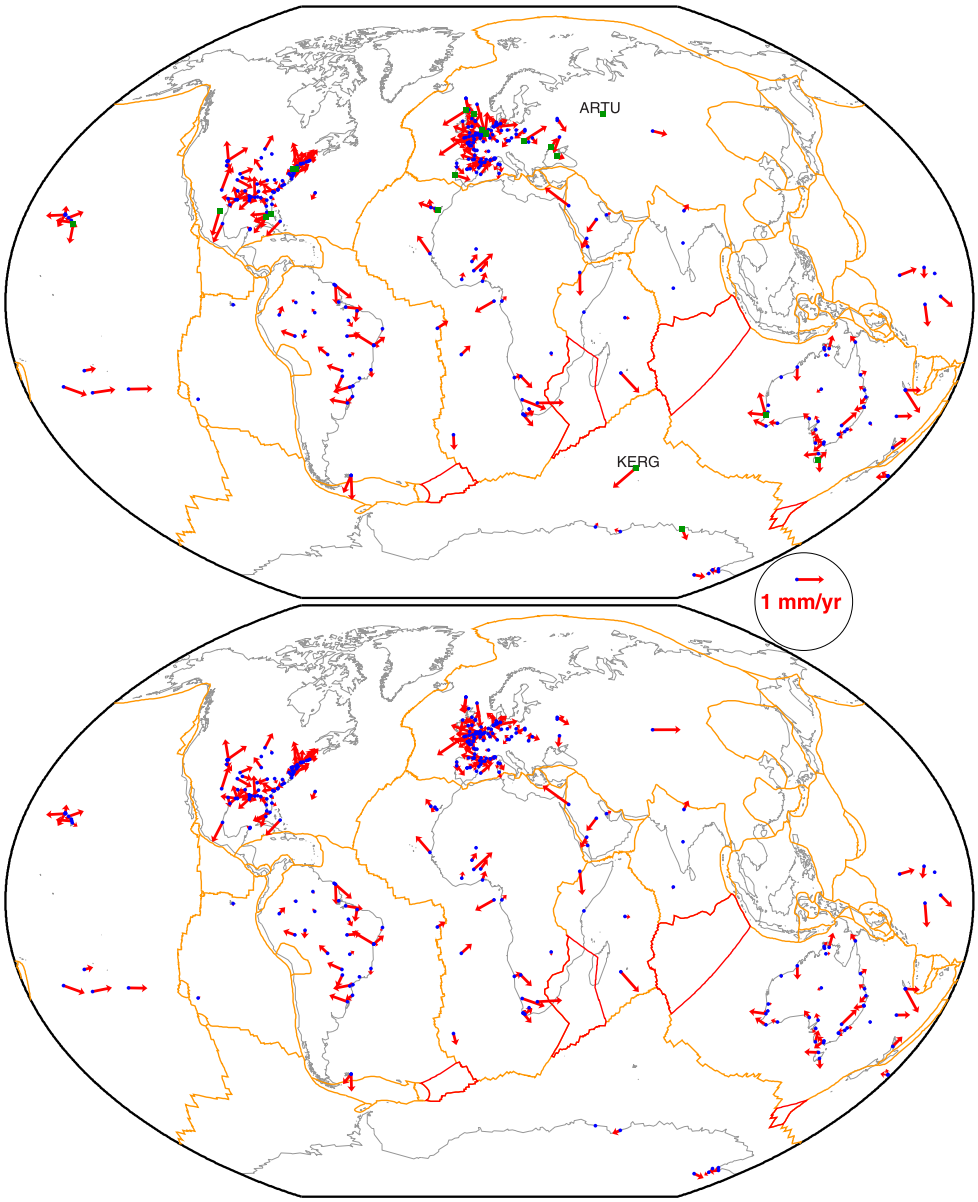

Figure 2. Post-fit residuals of the full set of 318 sites (top) and the filtered network of 297 sites (bottom), using the inversion model of eq. (2). Plate boundaries from Bird (2003) are shown in orange, and the four additional MORVEL plates (DeMets *et al.* 2010) are in red. Green squares in the top panel indicate the locations of the 21 rejected sites.

significant, and we therefore opted for a model without ORB. This model has also the advantage to accommodate geodetic practical applications in accessing the ITRF2014, especially for the implementation of national and continental reference frames where the rotation pole of a given plate is part of their definition. It is also worth noting that applying a PMM with an ORB different from zero leads to an undesirable and unjustified change of the vertical velocities.

Table 1 lists the ITRF2014 absolute rotation poles of the eleven plates, together with the WRMS values of the adjustment residuals for each one of the 11 plates, as well as the overall WRMS of the ITRF2014-PMM adjustment residuals which is at the level of 0.3 mm yr^{-1}. Fig. 3 illustrates the corresponding site residuals, which are in average at the same level of magnitude of 0.3 mm yr^{-1}. The listed rotation poles are defined relative to an NNR frame that has been propagated through the successive ITRF solutions (Altamimi *et al.* 2002, 2003, 2012).

We provide in the Supporting Information the following tables:

(i) Table S1: ITRF2014-PMM rotation pole Cartesian components in a computer readable file.

(ii) Table S2: list of the 297 selected sites and their horizontal velocities, together with one-sigma formal errors and their post-fit residuals.

(iii) Table S3: list of the 21 rejected sites and their horizontal velocities, together with their one-sigma formal errors and post-fit residuals as determined via the iterative inversion process where the normalized residual of any of the two horizontal components exceeded 3.0.

6 COMPARISON WITH ITRF2008-PMM AND GEOLOGICAL MODELS

In order to evaluate the level of agreement between ITRF2014-PMM and ITRF2008-PMM, we computed the differences between

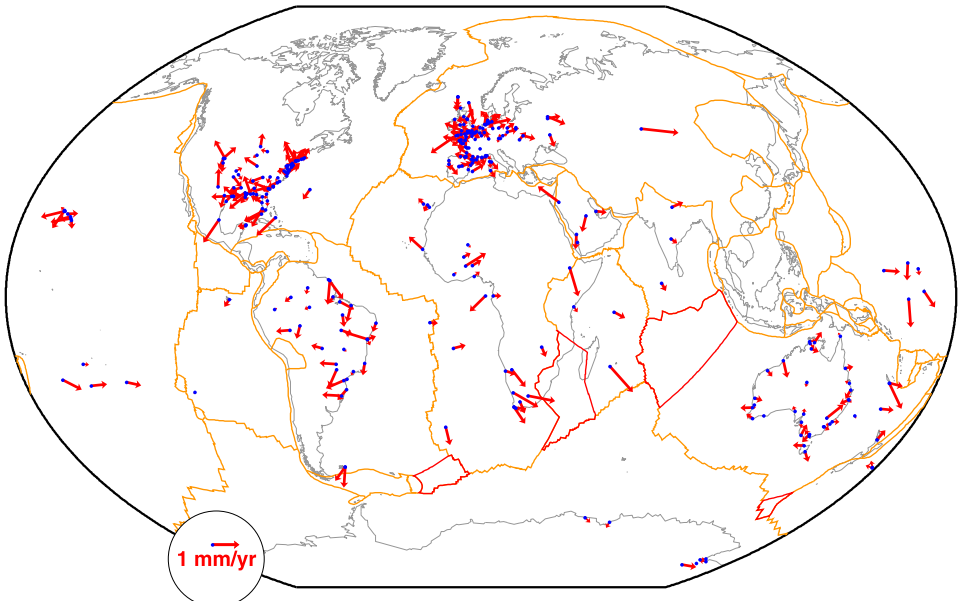

Figure 3. Post-fit site residuals of ITRF2014-PMM estimation, using the inversion model of eq. (1).

Table 1. Absolute plate rotation poles defining ITRF2014-PMM.

Plate	NS[a]	ω_x	ω_y	ω_z	ω	WRMS E	WRMS N
		(mas yr^{-1})			(° Ma^{-1})	(mm yr^{-1})	
ANTA	7	−0.248	−0.324	0.675	0.219	0.20	0.16
±		0.004	0.004	0.008	0.002		
ARAB	5	1.154	−0.136	1.444	0.515	0.36	0.43
±		0.020	0.022	0.014	0.006		
AUST	36	1.510	1.182	1.215	0.631	0.24	0.20
±		0.004	0.004	0.004	0.001		
EURA	97	−0.085	−0.531	0.770	0.261	0.23	0.19
±		0.004	0.002	0.005	0.001		
INDI	3	1.154	−0.005	1.454	0.516	0.21	0.21
±		0.027	0.117	0.035	0.012		
NAZC	2	−0.333	−1.544	1.623	0.629	0.13	0.19
±		0.006	0.015	0.007	0.002		
NOAM	72	0.024	−0.694	−0.063	0.194	0.23	0.28
±		0.002	0.005	0.004	0.001		
NUBI	24	0.099	−0.614	0.733	0.267	0.28	0.36
±		0.004	0.003	0.003	0.001		
PCFC	18	−0.409	1.047	−2.169	0.679	0.36	0.31
±		0.003	0.004	0.004	0.001		
SOAM	30	−0.270	−0.301	−0.140	0.119	0.34	0.35
±		0.006	0.006	0.003	0.001		
SOMA	3	−0.121	−0.794	0.884	0.332	0.32	0.30
±		0.035	0.034	0.008	0.008		
ITRF2014-PMM overall fit						0.26	0.26

[a] Number of sites.

the predicted velocities by the two models for the selected 297 sites plotted in Fig. 4. Note that the ITRF2008-PMM predicted velocities used here take into account its associated ORB whose magnitude is of the order of 0.4 mm yr^{-1}. As it can be seen from that figure, the largest differences are noted for plates ARAB, INDI and SOMA, each having a small number of sites. We discern also small changes for NOAM and SOAM that are reasonably within the overall uncertainty of 0.3 mm yr^{-1}. The high level of agreement between ITRF2014-PMM and ITRF2008-PMM is an indication of the overall stability of the orientation time evolution of the ITRF solutions and their successive alignments, at the level of (or better than) 0.3 mm yr^{-1}. This level of consistency is much higher than the consistency between available NNR geological models: NNR-NUVEL-1A (Argus & Gordon 1991) and NNR-MORVEL56 (Argus *et al.* 2011), as discussed by Altamimi *et al.* (2012).

7 CONCLUSIONS

Following strict criteria of site selection, satisfying the notion of rigid-plate motion hypothesis, at the level of (or better than) 0.3 mm yr^{-1} WRMS in average, we estimated a PMM for 11 major plates fully consistent with the ITRF2014. We demonstrated, through data analysis of multiple sub-networks of ITRF2014 velocity field that the ORB is strongly dictated by the selection of ITRF2014 sites used in the adjustment and varies, along its most-sensitive component, the Z-axis, between zero and more than 1 mm yr^{-1}. It is consequently hazardous to attribute any geophysical meaning to the estimated ORB, although one would expect a non-zero translational rate between the ITRF2014 origin and the origin of tectonic plate motions (i.e. the residual centre of surface lateral figure (Blewitt 2003)).

Based on several geophysical and statistical criteria, the ITRF2014-PMM was adjusted to the velocity field of a network of 297 ITRF2014 sites and comprises rotation poles for eleven plates intended for geophysical and operational geodetic applications. Using the same filtered network of 297 sites, we found in particular that the estimated ORB is statistically not far from zero at the 2-sigma level, but also according to the F-ratio test we applied to the results of both adjustments, with and without the ORB.

The selected velocity field of 297 sites, and consequently the corresponding ITRF2014-PMM may be slightly but significantly contaminated by GIA, depending on site locations. Therefore it would not be optimal to subtract PMM predictions from a velocity field in order to investigate GIA deformations. As we previously and extensively investigated the GIA impact on PMMs in Altamimi *et al.* (2012), we did not repeat this study here, although we conducted some tests by subtracting GIA predictions of different models before the inversions that led to the same results and conclusions as in

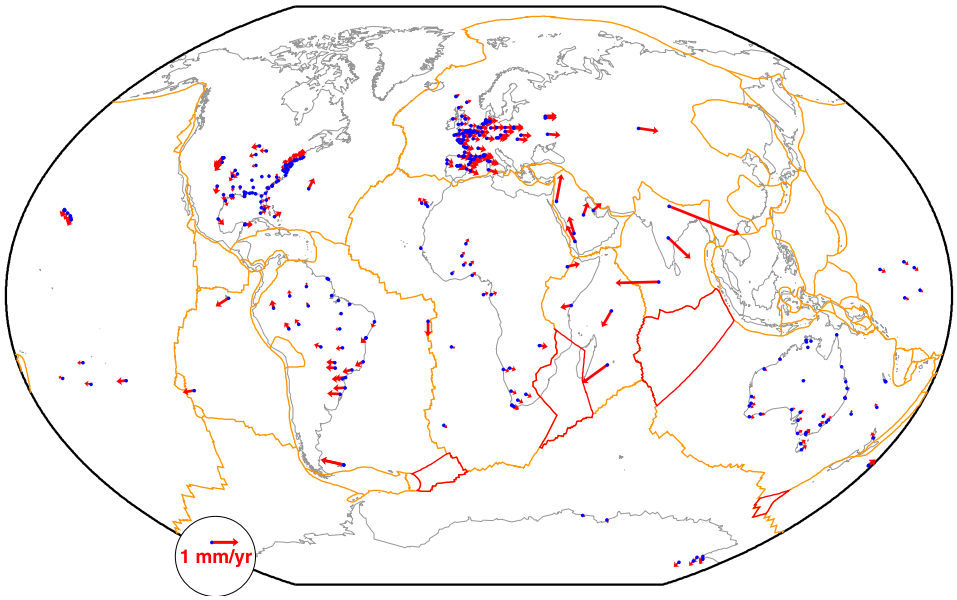

Figure 4. Differences of predicted velocities between ITRF2014-PMM and ITRF2008-PMM.

Altamimi *et al.* (2012). In short, none of the currently existing GIA models would improve the PMM fit (i.e. decreasing the residuals and WRMS) if site velocities were corrected by GIA model predictions. It is also worth mentioning that the current ice melting might have a significant secular signal that needs to be addressed in future work.

ACKNOWLEDGEMENTS

The International Terrestrial Reference Frame (ITRF) is the result of a global collaboration of hundreds of institutions around the world: from the build-up of geodetic observatories, satellite missions, data collection, analysis and combination, to the ITRF generation, thanks to the investment of national mapping agencies, space agencies, universities and research institutes. The ITRF activities are funded by the Institut national de l'information géographique et forestière (IGN), France, and partly by Centre National d'Etudes Spatiales (CNES). We thank Corné Kreemer for providing the strain map model, and Jean-Mathieu Nocquet for useful discussion. We acknowledge helpful comments and suggestions provided by two anonymous reviewers which improved the content of this paper.

REFERENCES

Altamimi, Z. & Boucher, C., 2002. The ITRS and ETRS89 relationship: new results form ITRF2000, in *Proceedings of the EUREF Symposium,* Dubrovnik, 16–18 May 2001, Verlag des Bundesamts für Kartographie und Geodäsie, Frankfurt am main.

Altamimi, Z., Sillard, P. & Boucher, C., 2002. ITRF2000: a new release of the International Terrestrial Reference Frame for Earth science applications, *J. geophys. Res.,* **107**(B10), 2214, doi:10.1029/2001JB000561.

Altamimi, Z., Sillard, P. & Boucher, C., 2003. The impact of a no-net-rotation condition on ITRF2000, *Geophys. Res. Lett.,* **30**(2), 1064, doi:10.1029/2002GL016279.

Altamimi, Z., Métivier, L. & Collilieux, X., 2012. ITRF2008 plate motion model, *J. geophys. Res.,* **117,** doi:10.1029/2011JB008930.

Altamimi, Z., Rebischung, P., Métivier, L. & Collilieux, X., 2016. ITRF2014: a new release of the International Terrestrial Reference Frame modeling nonlinear station motions, *J. geophys. Res.,* **121,** doi:10.1002/2016JB013098.

Argus, D.F. & Gordon, R.G., 1991. No-net-rotation model of current plate velocities incorporating plate motion model NUVEL-1, *Geophys. Res. Lett.,* **18,** 2038–2042.

Argus, D.F. & Gordon, R.G., 1996. Tests of the rigid-plate hypothesis and bounds on intraplate deformation using geodetic data from very long baseline interferometry, *J. geophys. Res.,* **101,** 13 555–13 572.

Argus, D.F., Gordon, R.G., Heflin, M.B., Ma, C., Eanes, R.J., Willis, P., Peltier, W.R. & Owen, S.E., 2010. The angular velocities of the plates and the velocity of Earth's centre from space geodesy, *Geophys. J. Int.,* **180**(3), 916–960.

Argus, D.F., Gordon, R.G. & DeMets, C., 2011. Geologically current motion of 56 plate relative to the no-net-rotation reference frame, *Geochem. Geophys. Geosyst.,* **12,** Q11001, doi:10.1029/2011GC003751 .

Bird, P., 2003. An updated digital model of plate boundaries, *Geochem. Geophys. Geosyst.,* **4**(3), 1027, doi:10.1029/2001GC000252.

Blewitt, G., 2003. Self-consistency in reference frames, geocenter definition, and surface loading of the solid Earth, *J. geophys. Res.,* **108**(B2), 2103, doi:10.1029/2002JB002082.

Blewitt, G. & Lavallée, D., 2002. Effect of annual signals on geodetic velocity, *J. geophys. Res.,* **107**(B7), 2145, doi:10.1029/2001JB000570.

Blewitt, G., Kreemer, C., Hammond, W. & Goldfarb, J.M., 2013. Terrestrial reference frame NA12 for crustal deformation studies in North America, *J. Geodyn.,* **72,** 11–24.

DeMets, C., Gordon, R.G., Argus, D.F. & Stein, S., 1990. Current plate motions, *J. geophys. Res.,* **101,** 425–478.

DeMets, C., Gordon, R.G., Argus, D.F. & Stein, S., 1994. Effect of recent revisions of the geomagnetic reversal timescale on estimates of current plate motions, *Geophys. Res. Lett.,* **21**(20), 2191–2194.

DeMets, C., Gordon, R.G. & Argus, D.F., 2010. Geologically current plate motions, *Geophys. J. Int.,* **181**(1), 1–80.

Herring, T.A. *et al.*, 2016. Plate Boundary Observatory and related networks: GPS data analysis methods and geodetic products, *Rev. Geophys.,* **54,** 759–808.

Kogan, M.G. & Steblov, G.M., 2008. Current global plate kinematics from GPS (1995–2007) with the plate- consistent reference frame, *J. geophys. Res.,* **113,** B04416, doi:10.1029/2007JB005353.

Kreemer, C., Blewitt, G. & Klein, E.C., 2014. A geodetic plate motion and Global Strain Rate Model, *Geochem. Geophys. Geosyst.,* **15,** 3849–3889.

Lambeck, K., Rouby, H., Purcell, A., Sun, Y. & Sambridge, M.M., 2014. Sea level and global ice volumes from the Last Glacial Maximum to the Holocene, *Proc. Natl. Acad. Sci. USA,* **111**(43), 15 296–15 303.

Lambeck, K., Purcell, A. & Zhao, S., 2017. The North American Late Wisconsin ice sheet and mantle viscosity from glacial rebound analyses, *Quat. Sci. Rev.,* **58,** 172–210.

Nocquet, J.-M., Calais, E., Altamimi, Z., Sillard, P. & Boucher, C., 2001. Intraplate deformation in western Europe deduced from an analysis of the ITRF97 velocity field, *J. geophys. Res.,***106**(B6), 11 239–11 257.

Peltier, W.R., Argus, D.F. & Drummond, R., 2015. Space geodesy constrains ice age terminal deglaciation: the global ICE-6G_C (VM5a) model, *J. geophys. Res.,* **120,** 450–487.

Sillard, P. & Boucher, C., 2001. Review of algebraic constraints in terrestrial reference frame datum definition, *J. Geod.,* **75,** 63–73.

SUPPORTING INFORMATION

Supplementary data are available at *GJI* online.

Table S1. ITRF2014-PMM rotation pole Cartesian components in DEG/My.

Table S2. Sites and their horizontal velocities used in the rotation poles estimation together with their one-sigma formal errors and post-fit residuals.

Table S3. The 21 rejected sites and their horizontal velocities, together with their one-sigma formal errors and post-fit residuals.

Please note: Oxford University Press is not responsible for the content or functionality of any supporting materials supplied by the authors. Any queries (other than missing material) should be directed to the corresponding author for the paper.